Journal of Power Sources 261 (2014) 86–92

Contents lists available at ScienceDirect

Journal of Power Sources

journal homepage: www.elsevier.com/locate/jpowsour

Effect of the chemical termination of conductive diamond substrate on the resistance to carbon monoxide-poisoning during methanol oxidation of platinum particles

Tanța Spătaru [a], Petre Osiceanu [a], Mihai Anastasescu [a], Greta Pătrinoiu [a], Cornel Munteanu [a], Nicolae Spătaru [a,*], Akira Fujishima [b]

[a] Institute of Physical Chemistry "Ilie Murgulescu", 202 Spl. Independenței, 060021 Bucharest, Romania
[b] Tokyo University of Science, 1-3 Kagurazaka, Shinjuku-ku, Tokyo 162-8601, Japan

HIGHLIGHTS

- Pt was electrodeposited on conductive diamond substrates annealed in H_2 or O_2 stream.
- Hydrogenated BDD support enables enhanced specific surface area of Pt particles.
- Oxidized BDD substrate renders Pt more resistant to fouling during CH_3OH oxidation.
- CO oxidative desorption occurs more readily when Pt is deposited on oxidized BDD.

ARTICLE INFO

Article history:
Received 14 January 2014
Received in revised form
4 March 2014
Accepted 13 March 2014
Available online 21 March 2014

Keywords:
Oxidized boron-doped diamond
Methanol oxidation
Electrocatalysis
Platinum electrodeposition

ABSTRACT

Boron-doped diamond (BDD) films were annealed in hydrogen or oxygen streams and were further used as substrates for Pt electrochemical deposition. SEM and AFM measurements have shown that, from the point of view of the efficiency of noble metal utilization, a hydrogen-terminated diamond (HT-BDD) support is more convenient because it enables better dispersion and smaller size of the deposited particles. An enhancement of *ca.* 23% of the electrocatalyst specific surface area was observed for Pt/HT-BDD, compared to the case of Pt deposited at oxygen-terminated diamond (OT-BDD). Nevertheless, it was found that when deposited on oxidized BDD, Pt particles are more resistant to fouling during methanol oxidation. Electrochemical oxidation of adsorbed carbon monoxide was investigated by anodic stripping voltammetry and it was demonstrated that the use of OT-BDD substrate facilitates oxidative desorption of CO from the platinum active sites. This behavior was tentatively ascribed to the high surface concentration of oxygenated carbon species, evidenced by XPS, which may act as oxygen donors and/or could partially weaken Pt–CO bonds, thus enabling easier CO eviction from the electrocatalyst surface.

1. Introduction

The ways to minimize the loadings of electrocatalytic noble metals without losing high catalytic activity is a research topic especially germane to the expected upsurge in high-efficiency fuel cells utilization [1–6]. In this respect, a particularly apposite approach is thought to be the deposition of the electrocatalyst as small particles on an electrically conductive, high surface area support which ensures a large number of reaction sites in a small volume (see Refs. [7,8] and references therein). Unfortunately, at the rather positive potential common for oxygen electrode, the most widely employed support materials for fuel cells (carbon blacks or other granular and pulverulent carbonaceous materials) can undergo irreversible oxidation at non-negligible rates, which renders the electrode less electrically conductive and can even deleteriously affect its mechanical integrity [9–11]. Even at the anode in direct methanol fuel cells, at less extreme potentials, these processes can be a problem because, no matter how slight, corrosion of the support can cause the metal electrocatalyst particles to be released from the surface, which can lead to the loss of electrical contact as well as agglomeration [12,13].

The outstanding chemical stability and robustness of conductive boron-doped diamond (BDD), together with its excellent electrochemical features provide a rationale for this material to be

* Corresponding author. Tel.: +40 21 224 8895; fax: +40 21 312 1147.
E-mail addresses: nspataru@icf.ro, n_spataru@yahoo.com (N. Spătaru).

http://dx.doi.org/10.1016/j.jpowsour.2014.03.044
0378-7753/

considered highly suitable for being used as substrate for electrocatalysts in some fuel cell applications [14–17]. Promising electrochemical results have been reported for methanol oxidation at Pt and Pt-based alloy particles deposited on nonporous BDD films [18–23], but the effectiveness as a substrate of these films is limited by their low specific surface area. In an attempt to compensate for this drawback, boron-doped diamond particles obtained by mechanical crushing of freestanding BDD polycrystalline films were also used as catalyst support [24,25], but the cost for such powder is currently not sufficiently low for widespread utilization and the size of the BDD particles is still in the micrometric range.

However, undoped diamond nanoparticles are actually rather low in cost, being produced by detonation, and many successful efforts have been made to boron-dope these [26,27]. For instance, commercially available diamond nanoparticles (particle size, 5–6 nm) were doped and then used as substrate for the deposition of homogeneously dispersed Pt particles, with the size of 3–4 nm [28]. It is also worthy of note that particle diameters of 3.4 nm were recently reported for platinum deposited on diamond nanoparticles, quite comparable to those of 3.0 nm observed for commercial Pt/E-Tek catalyst [29]. Thus, there are reasons to believe that with diamond nanoparticles as support, and by using appropriate Pt deposition methods, it would be possible to obtain, at least for small-scale applications, highly active electrocatalytic materials at a reasonable price.

Unlike sp^2-type carbon supports, chemical or electrochemical oxidation of diamond leads only to the change of the hydrogen-terminated surface (which inherently appears since the films are grown under hydrogen plasma or in a hydrogen atmosphere) into an oxygen-terminated one, with negligible loss of material [30]. Furthermore, the types of stable C–O surface functional groups, *e.g.*, C–O–C, C=O, and C–OH, that can exist on oxidized diamond may not exist on the graphite surface to the same extent [31,32]. This feature could be important because it was shown that the presence of oxides or oxygenated functional groups on the carbonaceous substrate can strongly influence both the dispersion level and the activity of the electrocatalysts [33–35]. Recently, it has also been reported that, when deposited on oxide–carbon composites, platinum particles exhibit better resistance to carbon monoxide poisoning [36]. Boron-doped diamond is well known as an extremely suitable electrode material for many applications (see for example [37,38] and references therein) but lesser investigated is the effect of its surface termination on the electrochemical performances of deposited electrocatalysts.

The present work was aimed at studying the potential benefits of using oxygen-terminated conductive diamond as a substrate for platinum deposition, with an eye to fuel cell applications. Methanol and carbon monoxide oxidation in acidic media were used to assess the practical utility of Pt-modified oxidized BDD electrodes.

2. Experimental

For this study, highly boron-doped (*ca.* 10^{21} atoms cm^{-3}) polycrystalline diamond films grown on Si wafers by microwave plasma-assisted chemical vapor deposition were used as working electrodes for the electrochemical deposition of platinum particles. H_2PtCl_6 (*ca.* 40% Pt) and the pure gases (O_2, H_2, Ar, CO) were obtained from Fluka and Linde, respectively and were used as received. All the other compounds were of analytical reagent grade, and all the solutions were prepared using doubly distilled water.

The electrochemical experiments were performed at room temperature, under deaerated conditions, in a conventional three-electrode glass cell, by means of a PAR 273A potentiostat. A high surface platinum gauze and a Ag/AgCl electrode (in saturated KCl solution) were used as counter and reference electrodes, respectively. For CO stripping measurements, the electrolyte solution (0.5 M H_2SO_4) was purged with Ar for 30 min, and then carbon monoxide adsorption was carried out by bubbling CO into the solution for 15 min. Finally, argon was bubbled again for 30 min to remove dissolved CO. During the entire treatment, the potential of the electrode was kept constant (−0.25 V).

The morphology of the samples was investigated by scanning electron microscopy (SEM) with a high resolution microscope (Quanta 3D FEG with Everhart–Thornley secondary electron detector), and by atomic force microscopy (AFM) measurements performed in the non-contact mode by means of XE-100 apparatus from Park Systems. Topographical AFM images were taken over an area of 20 × 20 μm^2 and for appropriate display and subsequent statistical analysis of the data XEI (v.1.8.0) software was used. Surface analysis performed by X-Ray Photoelectron Spectroscopy (XPS) was carried out on a Quantera SXM equipment, with a base pressure in the analysis chamber of 10^{-9} Torr. The X-ray source was Al K_α radiation (1486.6 eV, monochromatized) and the overall energy resolution was estimated at 0.65 eV by the full width at half maximum of the Au $4f_{7/2}$ line. In order to take into account the charging effect on the measured binding energies (BE) the spectra were calibrated using the C1s line corresponding to the diamond core excitation (BE = 283.5 eV). To minimize the effect of inadvertent contamination of the samples, a *ca.* 0.5 nm-thick layer was removed from the surface by gentle argon ion etching (1 keV, 0.2 min).

Prior to platinum electrodeposition, the surface of the BDD electrodes was subjected either to a hydrogenation treatment or to an oxidation one, by using slightly modified versions of methods previously described in the literature [39]. Briefly, hydrogenation was performed by heating conductive diamond samples for 2 h in a hydrogen atmosphere at 900 °C, whereas oxidized surfaces were achieved by exposure to oxygen gas at 550 °C for 3 h. After these thermal treatments, the electrodes thus obtained (further denoted as HT-BDD and OT-BDD, respectively) were gradually cooled at room temperature and then used as substrates for Pt particles.

Platinum deposition was carried out from a 0.5 M H_2SO_4 + 4.8 mM H_2PtCl_6 solution, by applying several consecutive potentiostatic pulses of two seconds' duration each (applied potential, −0.1 V), and the Pt loading was then calculated from the cathodic charge integrated during electrodeposition. Before further experiments, all Pt-modified diamond electrodes (Pt/HT-BDD and Pt/OT-BDD) were thoroughly washed with bidistiled water and then successive cyclic voltammograms were recorded in 0.5 M H_2SO_4 (potential range, −0.25 V–1.25 V; sweep rate, 50 mV s^{-1}), until a stable response was obtained (*ca.* 10 cycles).

3. Results and discussion

It is reasonable to assume that in order to straightforwardly put into evidence the effect of the oxygen-terminated diamond substrate on the electrochemical behavior of platinum particles, Pt/OT-BDD electrodes should be compared on a relative basis with those obtained by depositing similar amounts of platinum on an oxygen-free BDD surface. Although, due to the high dissociation energy of C–H chemisorbed bonds, hydrogenated as-deposited diamond is generally regarded as stable toward adsorption of atmospheric gases, it was found that, after a more or less prolonged exposure to air, the presence of a certain amount of oxygen on the surface cannot be avoided [40]. Complete removal of oxygenated species requires hydrogen-plasma treatments [41] but more accessible methods, such as strong cathodic polarization in acidic aqueous media [42,43] or thermal treatments in hydrogen atmosphere [39], have also been successfully used in order to achieve an overwhelming majority of C–H bonds on the diamond surface. For the

present work HT-BDD and OT-BDD supports were prepared by annealing BDD samples in hydrogen and oxygen streams, respectively (see Experimental Section). It is worth noting that such thermal treatments can also be easily employed for purposeful modification of the surface of conductive diamond powder supports, which, for obvious experimental reasons, would be more difficult to achieve by using electrochemical or plasma-based procedures. Thus, there are reasons to believe that the results of this investigation could provide a basis for additional experiments involving practical electrocatalyst supports for fuel cells.

Earlier studies concerning the effect of the chemical termination on the electrochemistry of diamond films have shown that redox species with negative charge are very sensitive to the presence of oxygen-containing surface groups [41,44,45]. Therefore cyclic voltammetry in a 0.5 M H_2SO_4 + 1 mM $K_4Fe(CN)_6$ solution was used for assessing the effectiveness of the above pre-treatments, typical results being shown in Fig. 1. Ere this, the surface of the investigated electrodes was analyzed by XPS and the corresponding narrow-scan spectra in the O 1s region are given in the inset from Fig. 1. Without any pre-treatment, a *ca.* 110 mV anodic-cathodic peak separation (ΔE_p) was observed at the BDD electrode (curve 1 from Fig. 1) which dovetails with a quasi-reversible electron transfer. As curve 2 shows, at HT-BDD electrodes ΔE_p slightly decreases suggesting that the apparent electron transfer at the diamond surface was somewhat accelerated by the hydrogenation treatment. Conversely, at OT-BDD a much higher peak separation (*ca.* 580 mV) was obtained (curve 3) which clearly indicates a significant decrease in the heterogeneous electron transfer rate constants. These results were not unexpected because a similar behavior was previously reported for electrochemically oxidized and for oxygen-plasma treated BDD and was ascribed to the fact that oxygen species from the diamond surface can act as repulsive sites with respect to the redox species with negative charge [31,41]. Actually, as the XPS analysis demonstrate (see the inset in Fig. 1), compared to untreated BDD, thermal oxidation leads to an increase of nearly 3.5 times of the oxygen surface concentration, whereas hydrogenation results in its slight decrease (with less than 15%), in line with the corresponding variation of ΔE_p evidenced by cyclic voltammetry.

Pre-treated BDD samples were further used as substrate for Pt electrochemical deposition and the behavior of the electrodes thus obtained (Pt/HT-BDD and Pt/OT-BDD) was firstly gauged by running several consecutive cyclic voltammetric experiments, until a stable response was recorded (see Experimental Section). After stabilization, the surface of the Pt-modified BDD electrodes was examined by SEM, and Fig. 2 shows characteristic micrographs obtained both for Pt/HT-BDD (Fig. 2(a)) and Pt/OT-BDD (Fig. 2(b)) with similar platinum loadings (40.4 and 40.8 μg cm^{-2}, respectively), together with the corresponding voltammetric patterns. It appears that, compared to oxidized BDD, the use of an HT-BDD substrate enables a more even spread and a smaller average size (*ca.* 200 nm) of the deposited Pt particles, although the presence of aggregates is also observed. The less uniform distribution of the particles across the surface of OT-BDD and the wider variation range of their size (Fig. 2(b)) can be plausibly ascribed to the fact that active sites at which $PtCl_6^{2-}$ ions reduction occurs are partially blocked by oxygen-containing groups, as previously postulated for BDD substrates oxidized by prolonged anodic treatments (see Ref. [46] and references therein). Due to this blockage, further Pt deposition will take place more readily on already deposited particles which accounts for the higher tendency toward large cluster

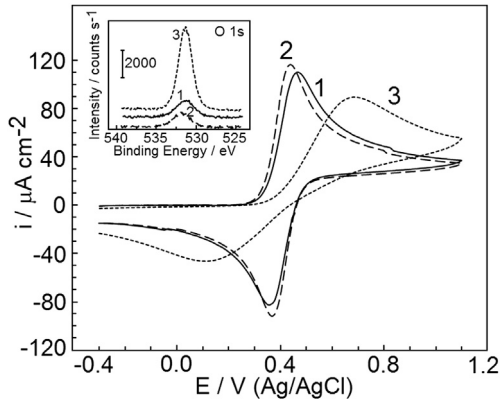

Fig. 1. Cyclic voltammograms recorded in a 0.5 M H_2SO_4 + 1 mM $K_4Fe(CN)_6$ solution (sweep rate, 50 mV s^{-1})for untreated BDD (1), HT-BDD (2) and OT-BDD (3) electrodes. Inset: corresponding narrow-scan XPS spectra in the O 1s region.

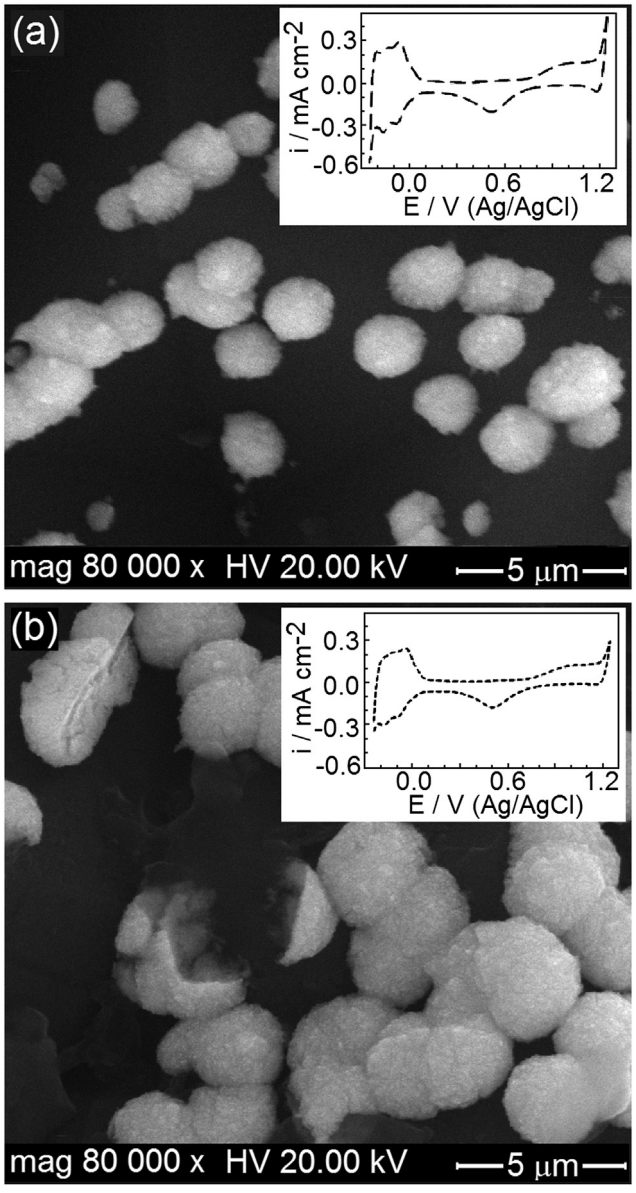

Fig. 2. Characteristic SEM micrographs for Pt/HT-BDD (a) and Pt/OT-BDD (b) electrodes recorded after stabilization of the voltammetric response. Insets: corresponding stable cyclic voltammograms recorded in 0.5 M H_2SO_4 at a sweep rate of 50 mV s^{-1}. Platinum loadings (μg cm^{-2}): (a) 40.4; (b) 40.8.

formation evidenced for Pt/OT-BDD electrodes by SEM measurements (Fig. 2(b)).

As insets from Fig. 2 demonstrate, the shape of the voltammetric response recorded for both types of electrodes after stabilization is typical for the behavior of platinum in acidic media, which enables the estimation of the active surface area of the electrocatalyst from the charge associated with hydrogen adsorption, corrected for that of the double layer. Thus, integration of the cathodic charge within the potential range −0.2 to 0.1 V yielded values of the hydrogen adsorption charge of *ca.* 90.7 and *ca.* 74.4 μC cm^{-2} for Pt/HT-BDD and Pt/OT-BDD, respectively. By assuming a value of 0.21 mC cm^{-2} for smooth platinum surface [47] and by taking into consideration the corresponding values of the platinum loading, specific surface areas of *ca.* 1.07 and *ca.* 0.87 m^2 g^{-1} can be roughly estimated for Pt particles supported on HT-BDD and OT-BDD. These values are well below those required for practical applications, which is obviously the result of the relatively low specific surface area of the diamond film. However, the above findings are noteworthy because they indicate that, in terms of efficiency of noble metal utilization, HT-BDD is better suited to be used as support for the electrocatalyst.

The effect of the substrate pre-treatment on the morphology of the platinum deposit was also examined by AFM and, as typical images from Fig. 3 illustrate, the results corroborate the conclusions

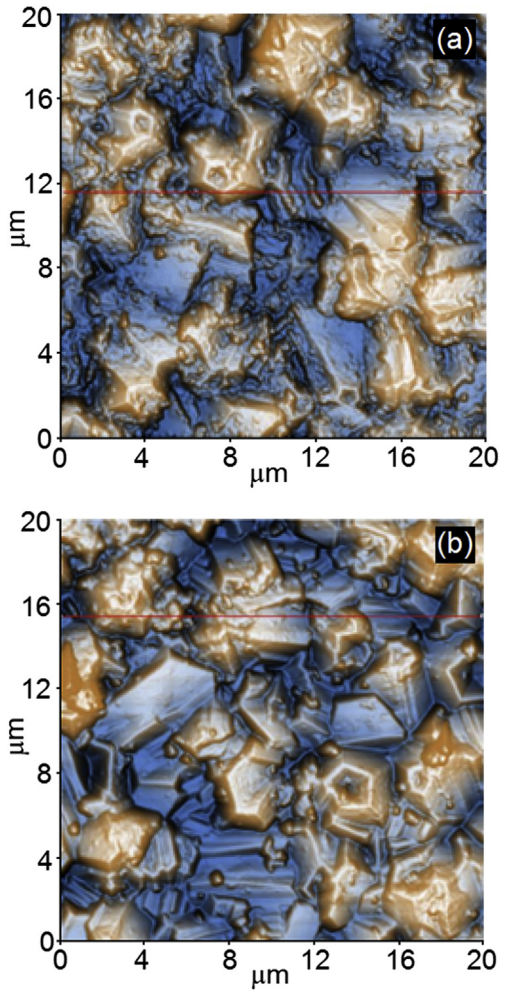

Fig. 3. AFM images of Pt/HT-BDD (a) and Pt/OT-BDD (b) electrodes recorded after stabilization of the voltammetric response. Platinum loadings (μg cm^{-2}): (a) 40.6; (b) 40.3.

of the SEM investigation suggesting that the use of a hydrogenated BDD substrate enables more uniform distribution of electrodeposited Pt particles. Interestingly, statistical analysis of the AFM results yielded for the two types of electrodes different kurtosis (R_{ku}) parameters. Thus, a value of 3.16 was found for Pt/HT-BDD, very close to that corresponding to a perfectly random surface (R_{ku} = 3), indicating a rather Gaussian surface distribution. Conversely, the higher value observed for Pt/OT-BDD (R_{ku} = 5.11) attests preferential agglomeration of electrocatalyst particles [48], in agreement with the proclivity towards cluster formation evidenced by SEM.

XPS was employed in order to analyze the surface of the Pt-modified pre-treated BDD electrodes and Fig. 4 shows narrow-scan spectra in the C 1s and Pt 4f regions, both for Pt/HT-BDD (a, b) and Pt/OT-BDD (c, d). It was observed that, for hydrogenated BDD, C 1s core level spectrum could be deconvoluted into three peaks (Fig. 4(a)). The most intense peak (at 283.5 eV) is characteristic to bulk diamond, *i.e.* carbon bonded only to carbon. Concerning the second peak, with lower intensity, the assigned value of the binding energy (BE, 284.9 eV) revealed the presence on the surface of adventitious carbon from the ambient, which can not be avoided without taking special precautions during measurements and samples handling [49]. The third peak, at even higher BE (286.5 eV), can be ascribed to the presence of carbon singly bonded to oxygen (C—OH and C—O—C) [41] and the relative surface concentration of these oxygenated species was found to be of *ca.* 2.4%.

For Pt/OT-BDD electrodes, high resolution spectra (Fig. 4(c)) exhibited an additional peak (BE, *ca.* 288.4 eV) attributed to C═O groups [45] (relative surface concentration, 2.6%), together with an enhancement of the peak corresponding to carbon singly bonded to oxygen (up to 6.5%). It therefore appears that the overall surface concentration of oxygenated carbon species is *ca.* 3.7 times higher for Pt/OT-BDD electrodes than for the Pt/HT-BDD ones, in good agreement with the results of XPS measurements in the O 1s region (see above).

In both cases, deconvoluted Pt 4f spectra put into evidence elemental platinum only. It was observed that, compared to the less intense doublet (BE, 71.3 and 74.6 eV) which is typical of the presence of Pt particles, the more intense one is shifted towards lower binding energy values, which is a characteristic of platinum metallic clusters [50]. In terms of relative surface concentration, Pt clusters prevailed (*ca.* 65% for Pt/HT-BDD and *ca.* 80% for Pt/OT-BDD), whereas Pt particles concentration was always lower (*ca.* 35% and *ca.* 20%, respectively). These findings are in line with the higher tendency for cluster formation evidenced by SEM for OT-BDD-supported platinum.

In order to check whether or not BDD pre-treatments affect in any way the electrocatalytic activity of supported platinum, methanol anodic oxidation in acidic media was chosen as a test-reaction. Long-term polarization measurements were performed in a 0.5 M H_2SO_4 + 2.46 M CH_3OH solution and Fig. 5 shows typical chronoamperometric curves recorded for electrodes with similar platinum loadings at an applied potential of 0.55 V. For a more straightforward comparison of the results on a relative basis, the oxidation current (I) was normalized by its maximum value (I_{max}). It was found that for short-time electrolysis (*ca.* 3 min) the time dependence of the current exhibits a rather sharp decrease for both types of electrodes, although after *ca.* 5 min this decrease becomes slower at Pt/OT-BDD. Thus, after 150 min of continuous polarization, the oxidation current at Pt/HT-BDD electrodes reached *ca.* 13% of its initial value while that for Pt/OT-BDD decreased only to *ca.* 21% (curves 1 and 2, respectively). This is an indication of the fact that, when deposited on oxidized diamond, platinum is less sensitive to deactivation (*e.g.* via CO poisoning) during methanol oxidation in acidic media.

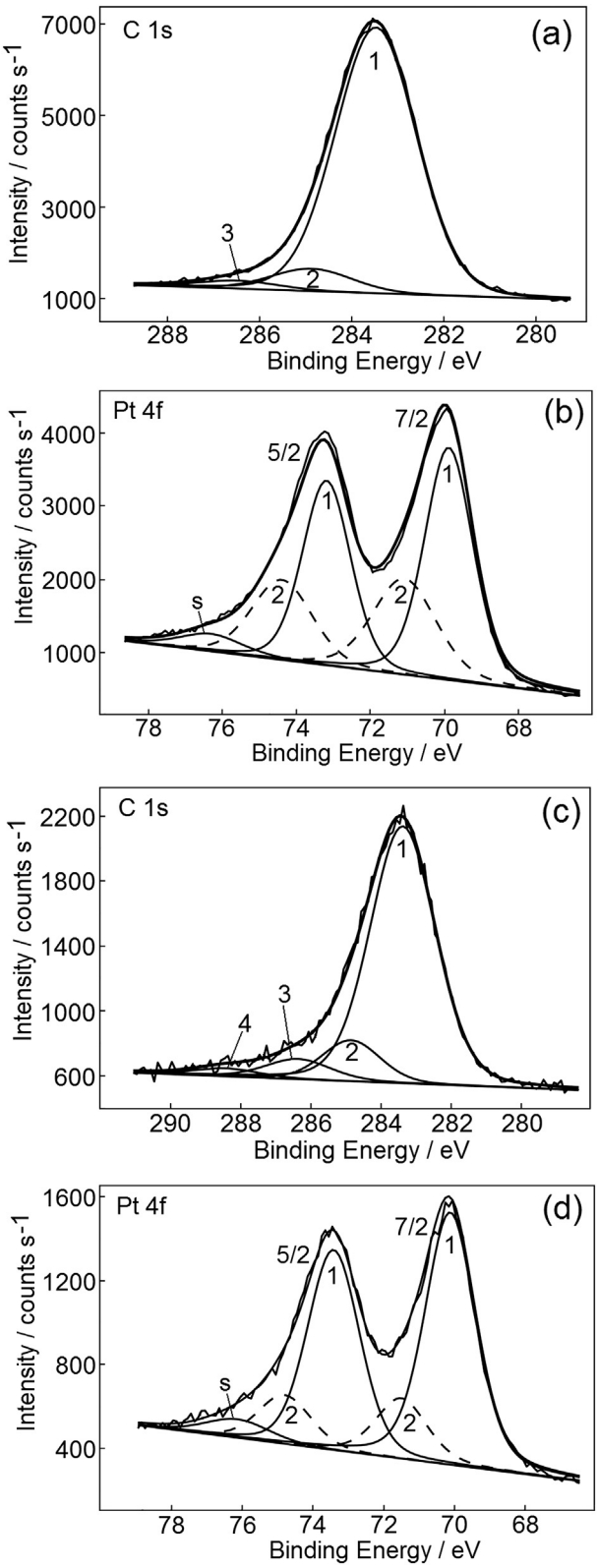

Fig. 4. Narrow-scan XPS spectra for Pt/HT-BDD (a,b) and Pt/OT-BDD (c,d) electrodes recorded after stabilization. In the C 1s region (a,c) the spectra were fitted by overlapping Gaussian–Lorentzian curves assigned to: (1) diamond; (2) adventitious carbon; (3) carbon singly bonded to oxygen; (4) C=O groups. In the Pt 4f region (b,d) of the spectra the doublets are assigned to: (1) Pt metallic clusters; (2) Pt particles. (The additional peak (s) corresponds to a satellite line which has the same binding energy as the primary $4f_{5/2}$ line but does not numerically alter the spectra.).

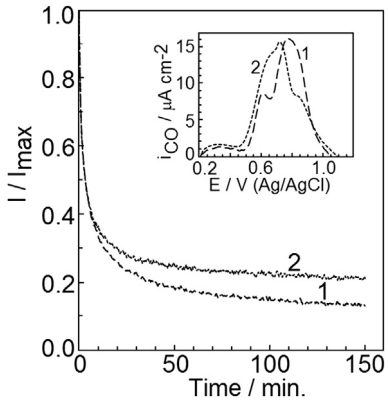

Fig. 5. Chronoamperograms for methanol oxidation recorded in a 0.5 M H_2SO_4 + 2.46 M CH_3OH solution at Pt/HT-BDD (1) and Pt/OT-BDD (2) electrodes (applied potential, 0.55 V). Inset: stripping voltammograms of adsorbed CO (corrected for the background current) recorded in 0.5 M H_2SO_4 at a sweep rate of 20 mV s^{-1} at Pt/HT-BDD (1) and Pt/OT-BDD (2) electrodes. (For other conditions, see text.) Platinum loadings, same as in Fig. 2.

To explain this behavior, the electrochemical oxidation of adsorbed CO was also investigated (see Experimental Section) and the inset from Fig. 5 shows typical anodic stripping voltammograms (corrected for the background current) for Pt/HT-BDD (curve 1) and Pt/OT-BDD (curve 2) electrodes with similar platinum loadings. To better emphasize the effect of the pre-treatments, the carbon monoxide oxidation current was always normalized to the active surface area of the platinum deposits, estimated by cyclic voltammetry (see above). Although the current responses are quite complex, it was found that the stripping charge which corresponds to CO oxidation is roughly the same in both cases (238 and 246 μC cm^{-2} for Pt/HT-BDD and Pt/OT-BDD, respectively), indicating a rather similar surface coverage of the platinum active sites. Nevertheless, at Pt/OT-BDD the CO stripping peak is slightly shifted towards lower potential values (with *ca.* 60 mV), supporting the conclusion that, when the electrocatalyst is deposited on oxidized BDD, the overall process of CO anodic oxidation is facilitated to a certain extent.

Anodic oxidation of irreversibly adsorbed carbon monoxide (*i.e.*, in the absence of solution-phase CO) at platinum electrodes has received substantial attention in the literature. Depending on the accumulation potential, several peaks (usually intermingled) were observed in stripping voltammetry, ascribed to the contribution to the overall oxidation process of CO species differently bound to Pt active sites [36,51–54]. Some details of the reaction pathway are still controversial but it was shown that CO stripping is best described by a Langmuir–Hinshelwood mechanism, notwithstanding that, in many cases, the voltammograms also exhibited a well-defined prepeak for which different mechanisms have been hypothesized (see Ref. [55] and references therein). Although the particular binding geometry of the different CO adsorbed species responsible for the multiplicity of electrooxidation peaks remains somewhat abstruse, it is widely accepted that two main forms are involved in the overall process: a “weakly adsorbed” one which is oxidized at lower potential (in the so-called preoxidation region) and a “strongly adsorbed” state of the CO which is oxidized at higher potentials (usually higher than *ca.* 0.6 V vs. reversible hydrogen electrode) [53]. Despite the fact that the shape of the voltammetric responses corresponding to the oxidation of differently adsorbed CO species might not be always symmetrical, it was previously shown that the charge associated to them could be reliably estimated by deconvoluting the background-corrected stripping voltammograms into Gaussian peaks [56,57]. In line

with these findings, the voltammetric responses of the Pt-modified BDD electrodes were fitted by assuming four overlapping peaks, as illustrated in Fig. 6. A single broad peak (labeled I) was associated with the preoxidation region, whereas at potential values higher than *ca.* 0.45 V the stripping voltammograms were characterized by three merging peaks (labeled II, III, and IV). Experimental and calculated data were in excellent agreement both for Pt/HT-BDD ($R^2 = 0.9995$) and Pt/OT-BDD ($R^2 = 0.9993$), and the corresponding peak potentials were found to be 0.34 and 0.33 V for peaks I, 0.60 and 0.62 V for peaks II, 0.76 and 0.74 for peaks III, and 0.86 V for peaks IV (see Fig. 6(a) and (b)). Inferring mechanistic details concerning CO oxidation is not an easy task and was beyond the scope of the present work. We should note, however, that the closeness of the peak potentials for each of the four peaks strongly suggests that the processes responsible for their occurrence are, at both types of electrodes, very similar. After deconvolution, the integration of the charge under these peaks has shown that at Pt/OT-BDD electrodes *ca.* 5.2% and *ca.* 34.3% of the total stripping charge is associated to CO oxidation within the range of peaks I and II respectively, whereas at Pt/HT-BDD the corresponding proportions are only of *ca.* 4.2% and *ca.* 16.5%. Conversely, in the latter case, a more important amount of CO is oxidized at higher potentials within the range of peaks III and IV, involving *ca.* 51.7% and *ca.* 27.6% of the total charge while, at Pt/OT-BDD electrodes, the corresponding percentages were found to be of *ca.* 38.3% and *ca.* 22.2%, respectively.

It is difficult to explain this behavior without further detailed work. Nevertheless, it seems reasonable to conjecture that there could be a small co-catalytic effect of the OT-BDD surface, resulting from the higher surface concentration of oxygenated carbon species. Due to their proximity to the Pt particles, these species could be available to act as oxygen donors and may assist in the oxidative desorption of the carbon monoxide. Another possibility is that CO adsorption at OT-BDD-supported platinum particles is somewhat weaker, simply because of the electrostatic repulsion exerted by these oxygenated species. Although these issues remain to be addressed, these results are noteworthy since they indicate that, in terms of readiness of CO desorption, there is a slight, but nonetheless significant, inherent advantage of the Pt/OT-BDD electrodes. For fuel cell applications, this feature may be important because it could provide a simple pathway for improving the resistance to CO poisoning of Pt particles during methanol anodic oxidation.

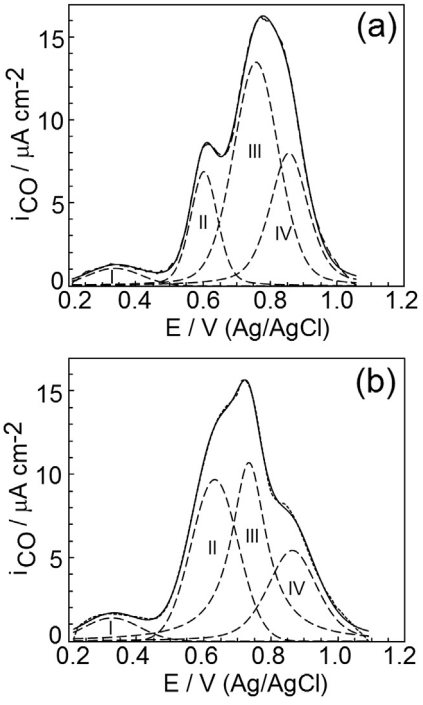

Fig. 6. Deconvolution of the anodic stripping voltammograms recorded at Pt/HT-BDD (a) and Pt/OT-BDD (b) electrodes during CO oxidative desorption. Solid lines represent voltammograms fitted by assuming four overlapping peaks (dashed lines).

4. Conclusions

In recent years much attention was given to the use of conductive diamond as support for electrocatalysts, triggered not only by the obvious advantages of this material (outstanding electrochemical features, excellent electrochemical and mechanical stability), but also by the promising results of the efforts to boron-dope inexpensive, commercially available, nanodiamond particles. This growing interest prompted us to investigate the effect of the oxygenated carbon species from the BDD surface on the electrochemical behavior and catalytic activity of deposited platinum particles.

In order to achieve the oxidation of the polycrystalline diamond surface, a thermal method was preferred which is also suitable for the modification of BDD powder surface. Oxygen-terminated BDD was further used as substrate for Pt electrochemical deposition. To better emphasize the effect of the chemical termination of the surface, electrodes obtained by depositing Pt on thermally hydrogenated BDD samples were also used, for comparison. SEM and AFM measurements have shown that, from the point of view of the efficiency of noble metal utilization, hydrogen-terminated BDD is more convenient because its use as a substrate enables better dispersion and smaller size of the deposited Pt particles. Thus, for HT-BDD-supported platinum, an enhancement of *ca.* 23% of the electrocatalyst specific surface area was evidenced by cyclic voltammetry, compared to Pt/OT-BDD electrodes. Conversely, long-term polarization experiments suggested that, when deposited on oxidized BDD, platinum particles are more resistant to fouling during methanol anodic oxidation. Electrochemical oxidation of adsorbed carbon monoxide was investigated by anodic stripping voltammetry and it was demonstrated that the use of an oxygen-terminated BDD substrate facilitates oxidative desorption of CO from the platinum active sites. This behavior was tentatively ascribed to the presence of a large amount of oxygenated carbon species which may act as oxygen donors and/or could partially weaken Pt–CO bonds, thus enabling easier CO eviction from the electrocatalyst surface.

This work was supported by a grant of the Romanian National Authority for Scientific Research, CNCS–UEFISCDI project number PN-II-ID-PCE-2011-3-0272. POS-CCE O 2.2.1 project INFRANANOCHEM-Nr. 19/01.03.2009 funded by EU (ERDF) and Romanian Government is also gratefully acknowledged for the XPS, AFM and SEM equipment.

References

[1] W. Vielstich, A. Lamm, H. Gasteiger, Handbook of Fuel Cells: Fundamentals, Technology, Applications, John Wiley & Sons, New York, 2003.
[2] S. Srinivasan, Fuel Cells: From Fundamentals to Applications, Springer, Heidelberg, 2006.
[3] E. Antolini, Mater. Chem. Phys. 78 (2003) 563–573.
[4] K.Y. Chan, J. Ding, J. Ren, S. Cheng, K.Y. Tsang, J. Mater. Chem. 14 (2004) 505–516.
[5] O.A. Petrii, J. Solid State Electrochem. 12 (2008) 609–642.
[6] J. Wu, X.Z. Yuan, J.J. Martin, H. Wang, J. Zhang, J. Shen, S. Wu, W. Merida, J. Power Sources 184 (2008) 104–119.
[7] H. Liu, C. Song, L. Zhang, J. Zhang, H. Wang, D.P. Wilkinson, J. Power Sources 155 (2006) 95–110.
[8] M.K. Debe, Nature 486 (2012) 43–51.

[9] E. Antolini, J. Mater. Sci. 38 (2003) 2995–3005.
[10] K.H. Kangasniemi, D.A. Condit, T.D. Jarvi, J. Electrochem. Soc. 151 (2004) E125–E132.
[11] C.H. Paik, T.D. Jarvi, W.E. O'Grady, Electrochem. Solid State Lett. 7 (2004) A82–A84.
[12] T.R. Ralph, M.P. Hogarth, Platin. Met. Rev. 46 (2002) 117–135.
[13] E. Antolini, Appl. Catal. B 88 (2009) 1–24.
[14] J. Wang, G.M. Swain, T. Tachibana, K. Kobashi, Electrochem. Solid State Lett. 3 (2000) 286–289.
[15] J. Wang, G.M. Swain, Electrochem. Solid State Lett. 5 (2002) E4–E7.
[16] G. Siné, I. Duo, B. El Roustom, G. Fóti, Ch Comninellis, J. Appl. Electrochem. 36 (2006) 847–862.
[17] F. Gao, N. Yang, C.E. Nebel, Electrochim. Acta (2013). http://dx.doi.org/10.1016/j.electacta.2013.09.005.
[18] K. Honda, M. Yoshimura, T.N. Rao, D.A. Tryk, A. Fujishima, K. Yasui, Y. Sakamoto, K. Nishio, H. Masuda, J. Electroanal. Chem. 514 (2001) 35–50.
[19] G. Siné, Ch Comninellis, Electrochim. Acta 50 (2005) 2249–2254.
[20] I. González-González, D.A. Tryk, C.R. Cabrera, Diam. Relat. Mater. 15 (2006) 275–278.
[21] G.R. Salazar-Banda, H.B. Suffredini, M.L. Calegaro, S.T. Tanimoto, L.A. Avaca, J. Power Sources 162 (2006) 9–20.
[22] G. Siné, D. Smida, M. Limat, G. Fóti, Ch Comninellis, J. Electrochem. Soc. 154 (2007) B170–B174.
[23] X. Lu, J. Hu, J.S. Foord, Q. Wang, J. Electroanal. Chem. 654 (2011) 38–43.
[24] G.R. Salazar-Banda, K.I.B. Eguiluz, L.A. Avaca, Electrochem. Commun. 9 (2007) 59–64.
[25] N. Spataru, X. Zhang, T. Spataru, D.A. Tryk, A. Fujishima, J. Electrochem. Soc. 155 (2008) B264–B269.
[26] Y. Shao, J. Liu, Y. Wang, Y. Lin, J. Mater. Chem. 19 (2009) 46–59.
[27] L. Cunci, C.R. Cabrera, Electrochem. Solid State Lett. 14 (2011) K17–K19.
[28] L. La-Torre-Riveros, E. Abel-Tatis, A.E. Mendez-Torres, D.A. Tryk, M. Prelas, C.R. Cabrera, J. Nanopart. Res. 13 (2011) 2997–3009.
[29] V. Celorrio, D. Plana, J. Florez-Montano, M.G. Montes de Oca, A. Moore, M.J. Lazaro, E. Pastor, D.J. Fermin, J. Phys. Chem. C 117 (2013) 21735–21742.
[30] M. Hupert, A. Muck, J. Wang, J. Stotter, Z. Cvackova, S. Haymond, Y. Show, G.M. Swain, Diam. Relat. Mater. 12 (2003) 1940–1949.
[31] H. Notsu, T. Tatsuma, A. Fujishima, in: A. Fujishima, Y. Einaga, T.N. Rao, D.A. Tryk (Eds.), Diamond Electrochemistry, BKC Inc., Tokyo, 2005.
[32] K. Nakagawa, M. Nishitani-Gamo, T. Ando, Int. J. Hydrogen Energy 30 (2005) 201–207.
[33] C.P. Burguete, A.L. Solano, F.R. Reinoso, C.S.M. Lecea, J. Catal. 115 (1989) 98–106.
[34] P.L. Antonucci, V. Alderucci, N. Giordano, D.L. Cocke, H. Kim, J. Appl. Electrochem. 24 (1994) 58–65.
[35] Y.F. Yang, Y.H. Zhou, J. Electroanal. Chem. 415 (1996) 143–152.
[36] B. Ruiz Camacho, C. Morais, M.A. Valenzuela, N. Alonso-Vante, Catal. Today 202 (2013) 36–43.
[37] A. Kraft, Int. J. Electrochem. Sci. 2 (2007) 355–385.
[38] G.R. Salazar-Banda, Y. Einaga, C.A. Martinez-Huitle, in: New Trends on the Boron-Doped PatentDiamond Electrode: From Fundamental Studies to Applications, International Journal of Electrochemistry, Hindawi Publishing Corporation, 2012.
[39] A. Laikhtman, A. Hoffman, Surf. Sci. 522 (2003) L1–L8.
[40] G. Piantanida, A. Breskin, R. Chechik, O. Katz, A. Laikhtman, A. Hoffman, C. Coluzza, J. Appl. Phys. 89 (2001) 8259–8264.
[41] I. Yagi, H. Notsu, T. Kondo, D.A. Tryk, A. Fujishima, J. Electroanal. Chem. 473 (1999) 173–178.
[42] H.B. Suffredini, V.A. Pedrosa, L. Codognoto, S.A.S. Machado, R.C. Rocha-Filho, L.A. Avaca, Electrochim. Acta 49 (2004) 4021–4026.
[43] L.S. Andrade, G.R. Salazar-Banda, R.C. Rocha-Filho, O. Fatibello-Filho, in: E. Brillas, C.A. Martinez-Huitle (Eds.), Synthetic Diamond Films: Preparation, Electrochemistry, Characterization, and Applications, John Wiley & Sons, Inc., Hoboken, 2011.
[44] H. Notsu, I. Yagi, T. Tatsuma, D.A. Tryk, A. Fujishima, Electrochem. Solid State Lett. 2 (1999) 522–524.
[45] H. Notsu, I. Yagi, T. Tatsuma, D.A. Tryk, A. Fujishima, J. Electroanal. Chem. 492 (2000) 31–37.
[46] M.C. Ribeiro, L.G. da Silva, P.T.A. Sumodjo, J. Braz. Chem. Soc. 17 (2006) 667–673.
[47] P.N. Ross Jr., J. Electrochem. Soc. 126 (1997) 67–77.
[48] D.J. Whitehouse, Handbook of Surface Metrology, Institute of Physics, Bristol, 1994.
[49] K.G. Saw, J. du Plessis, Mater. Lett. 58 (2004) 1344–1348.
[50] National Institute of Standards and Technology (NIST), X-ray Photoelectron Spectroscopy Database Version 4.0, NIST, Gaithersburg, 2008.
[51] F. Kitamura, M. Takahashi, M. Ito, Surf. Sci. 223 (1989) 493–508.
[52] A. Wieckowski, M. Rubel, C.J. Gutierrez, J. Electroanal. Chem. 382 (1995) 97–101.
[53] N.M. Markovic, B.N. Grgur, C.A. Lucas, P.N. Ross, J. Phys. Chem. B 103 (1999) 487–495.
[54] Y.Y. Tong, H.S. Kim, P.K. Babu, P. Waszczuk, A. Wieckowski, E. Oldfield, J. Am. Chem. Soc. 124 (2002) 468–473.
[55] P. Urchaga, S. Baranton, C. Coutanceau, G. Jerkiewicz, Langmuir 28 (2012) 13094–13104.
[56] V.A. Sethuraman, B. Lakshmanan, J.W. Weidner, Electrochim. Acta 54 (2009) 5492–5499.
[57] S. Balasubramanian, B. Lakshmanan, C.E. Hetzke, V.A. Sethuraman, J.W. Weidner, Electrochim. Acta 58 (2011) 723–728.